

Application of Full-Waveform Acoustic Borehole Logging to Detect and Characterize Rock Mass Fracture

Tartoussi Nourhan^{1,2}, Lataste Jean-François¹, Rivard Patrice², Barbosa Nicolás D.³

¹I2M /Bordeaux University

351 cours de la Libération 33405, Talence, France

nourhan.tartoussi@u-bordeaux.fr ; jean-francois.lataste@u-bordeaux.fr

² Department of Civil Engineering and Building Engineering /Sherbrooke University

2500 Bd de l'Université J1K 2R1, Sherbrooke, Canada

patrice.rivard@usherbrooke.ca

³ Institute of Earth Sciences/ University of Lausanne

Lausanne, Switzerland

nicolas.barbosa@unil.ch

Abstract - The characterization of discontinuities in the rock mass is very important to evaluate the global geomechanical properties of the mass, as it aims at solving problems in rock mechanics, such as the design of civil engineering structures, preventing landslides, etc. The presence of fracture affects the propagation of compression, shear, and surface waves that are recorded with acoustic borehole logging. To understand how filled fractures affect acoustic waves in a borehole environment, numerical simulations of full-waveform sonic response was performed using COMSOL Multiphysics software. This paper deals with two factors that can be used to quantify the transmission losses generated by fracture presence: velocity variation and amplitude attenuation (in the frequency domain) of P and S waves. In addition, the impact of multiple parameters of the discontinuity on transmission losses factors, such as fracture width, length, compression velocity, shear velocity, and the density of the fracture filling materials, were examined. S waves were found to be more sensitive to fracture characteristics. The influence of fracture length on compression and shear wavelength responses, as well as their relationship with P and S wave wavelengths, were underlined. We show that the velocity variation is more indicative of fracture width than the amplitude attenuation. These characteristics allow using shear and compression waves to characterize fractures.

Keywords: Fractures – Acoustic logging – Compression wave – Shear wave – Transmission losses factors.

1. Introduction

Rock masses are discontinuous, inhomogeneous, anisotropic [1]. Fractures play a critical role in reducing the underground bearing capacity, increasing the rock permeability, and reducing the factor of safety of rock slopes. Consequently, geotechnicians must evaluate the overall mechanical behavior of the rock mass based on the characterization of its components (rock matrix and the discontinuities) in any designs of civil or mining works.

Usually, geomechanical properties of rock masses are calculated from field measurements and core testing. However, the limitations of these techniques call for developing new methods that allow investigating larger volume, such as well-logging technologies in order to integrate the complexity of the natural environment. Acoustic well-logging tools are currently of great interest and are generally rather quick to implement at reasonable costs. They aim at detecting, locating, characterizing, and quantifying discontinuities, they allow multiplying the measurements in the rock mass in space and time. Therefore, they improve the knowledge of the rock because it allows going "beyond" the wall of the drilling. The approaches developed in applied geology with logging tools (borehole geophysics) have great potential to better take advantage of the boreholes [2-3-4-5-6].

Furthermore, during well-logging, the presence of fractures alters the wave propagation (compression, shear, and surface waves) because their speeds and amplitudes are affected by the path travelled and the interfaces encountered. As a result, understanding how fractures affect acoustic waveforms can help with fracture identification and characterization [7-8-9].

While the sensitivity of P-waves to fracture mechanical properties in sonic experiments has been previously addressed [10-11], this study focuses on the evaluation of the sensitivity of S-waves to the fracture mechanical properties (VP:

compression velocity, VS: shear velocity, RHO: density) and geometrical properties (e : width, L : length) when propagating in a borehole environment. The sensitivity of P-waves and S-waves will be analyzed and compared together. To do so, we simulated and compared the wave signals travelling across unfractured and fractured sections of a fluid-filled borehole.

This study is divided into three sections. We go through our numerical model, the main element of our parametric analysis, and our process for determining transmission loss factors in section two. The discussion of our results occurs in section three. In section four, conclusions are presented.

2. Methodology

2.1. Numerical simulation

To study the sensitivity of the width, the length, and the mechanical properties of a filled fracture on the full-wave sonic response, a finite element simulation was performed using COMSOL Multiphysics 5.6 (Structural mechanics and Acoustics modules) [12]. A planar axis-symmetric approach was used to simulate the propagation of acoustic waves in a borehole across a fracture cutting normal to the borehole axis (Fig.1). An elastic model was chosen considering the properties provided in Table 1. To prevent any spurious reflected waves generated by the model boundary, the outer limits were truncated with a perfectly matched layer (PML) absorbing boundaries [13] (Fig.1.b). We applied a Ricker wavelet with a core frequency of 20 kHz as the source. Signals were recorded over a 3ms record length by three receivers located 0.91m, 1.21m and 1.51m above the transmitter.

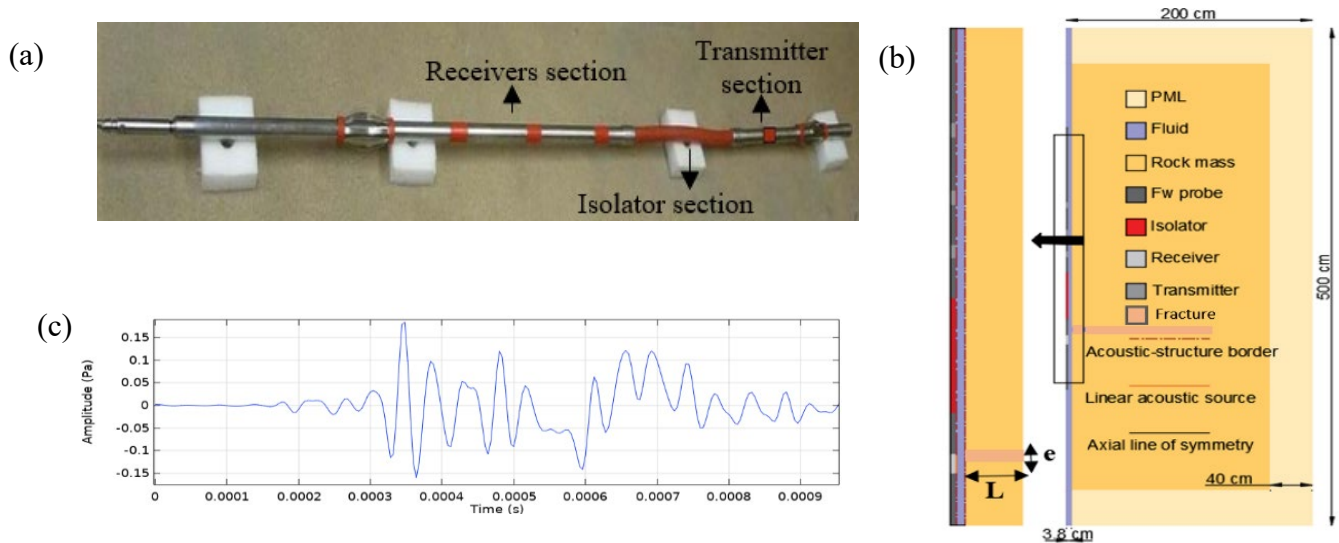


Fig. 1: (a) Full wave sonic probe. (b) Schematic diagram of the simulated model: borehole intersected by a horizontal fracture. The absorbing border of the perfectly matched layer (PML) is added to the model's boundary. (c) Plot showing a time-domain full-wave acoustic response.

Table 1: Reference material properties.

	VP (m/s)	VS (m/s)	RHO (kg/m ³)	e (cm)	L (cm)
Rock mass	6250	3700	3000	-	-
Fluid	1500	-	1000	-	-
Fracture	2000	750	1600	5	200

In addition, as indicated in Table 2, a parametric study was carried out while changing the geometrical and mechanical features of the fracture. Without considering the physical relationship between the fracture properties, we modified the value of each parameter independently.

Table 2: Geometrical and mechanical values of a fracture. Bold character represents the reference case properties.

	e (cm)	L (cm)	VP (m/s)	VS (m/s)	RHO (kg/m³)
Intervals	0.5-1-2- 5	1.5-10-15-20-40- 60-80- 200	1000- 2000 - 3000	500- 750 - 1250	1000- 1600 - 2200

To validate the numerical model, we simulate a unfractured model, and then compared the medium defined velocities V_M (VP and VS of rock mass presented in Table 1) with the calculated velocities V_C from FE computation for P and S waves. First, we separated the first arrivals of P and S waves from other types of waves. Second, we calculated the P and S waves phase velocities from the difference of the phase spectra $\Delta\varphi$ of the signals recorded at two receivers as [4]:

$$V_p(\omega); V_s(\omega) = \frac{\omega \Delta r}{\Delta \varphi(\omega)}; \left(\frac{m}{s}\right) \quad (1)$$

Where ω is the angular frequency and Δr is the distance between the two receivers.

The maximum error associated with our numerical model for VP and VS is about 1.5 %. The error was calculated based on Equation 2:

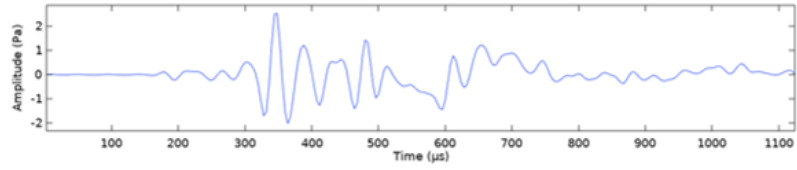
$$e_1 = 100 \left(\frac{V_M - V_C}{V_M} \right); (\%) \quad (2)$$

2.2. Quantification of transmission losses

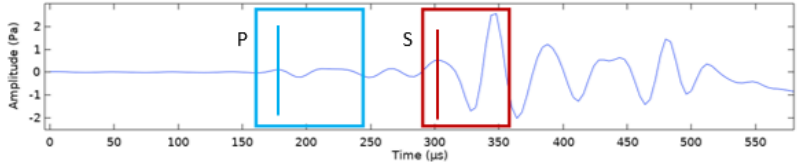
Two different models were tested. The first model presented an unfractured medium, while the second model represented a medium with a single fracture located between the transmitter and the receivers (0.4m above the transmitter). The unfractured model illustrates the borehole's undamaged sections and serves as a reference model for calculating time delays and amplitude decay in fractured sections. To study the influence of a fracture, we were interested to quantify the velocity attenuation and the amplitude decay of the first-cycle wavelet for P and S waves.

The procedure of determining the arrival times of P and S waves (dt) and the first wavelet amplitude in the frequency domain for the two types of waves (A) are briefly summarized in Fig. 2. First, we begin by obtaining the numerical receiver response in the time domain. Second, we specify the arrival time and interval of the first cycle wavelet of both types of waves (P and S). Third, we isolate the first arrival from the rest of the record using a half-cosine time window tapered at both ends of the first wavelet. Finally, we obtain the maximum amplitude in the frequency domain by applying the Fourier transform to the signal.

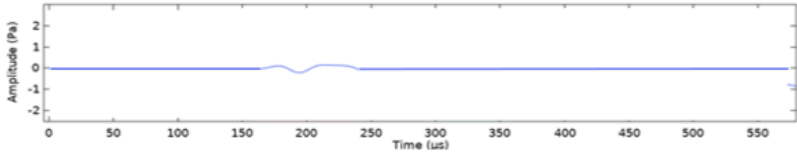
1. Extraction of the receiver's response from the numerical model.



2. Determination of the arrival time and the first wavelet of P and S waves,



3. Application time-windowing processes (Hanning) to separate the first wavelet of P and S-wave signals from the recorded signal.



4. Calculation of the first wavelet's amplitude in the frequency domain by applying the inverse of the Fourier transform.

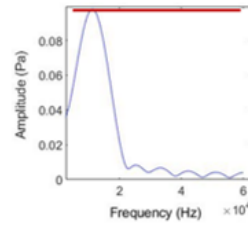


Fig. 2: Diagram shows the process of transmission loss factors quantification from fractured and unfractured models.

Furthermore, to quantify the transmission losses caused by discontinuities, two factors were calculated:

1. The velocity variation (VV) for P ($VV_{(P)}$) and S ($VV_{(S)}$) waves:

The medium velocities (P and S) of fractured and unfractured medium was calculated using Equation 3:

$$V = \frac{\Delta x}{dt - t_{borehole}}; \left(\frac{m}{s}\right) \quad (3)$$

Where Δx is the distance from the transmitter to the receiver (here we represent the results only for the first receiver located at an offset $\Delta x = 0.91m$), and $t_{borehole}$ is the time required for waves to travel directly through the borehole fluid (for a 7.62 cm diameter borehole and a 5.08 cm diameter of the probe $t_{borehole} = (d_{borehole} - d_{probe})/V_{fluid}$).

The velocity variation was computed using Equation 4:

$$VV = \frac{(V_{UF} - V_F) * 100}{V_{UF}}; (\%) \quad (4)$$

Where V_{UF} is the compression or shear velocity of the unfractured medium; V_F is the same for the fractured one.

2. The attenuation parameter (γ) for P ($\gamma_{(P)}$) and S ($\gamma_{(S)}$) waves:

The attenuation parameter was calculated following equation 5:

$$\gamma = -20 \text{ LOG} \left(\frac{A_F}{A_{UF}} \right); (dB) \quad (5)$$

Where A_F is the max amplitude of the signals (P and S) in the frequency domain for the fractured section; A_{UF} is the same for the intact medium.

As shown in Fig.3, the fracture length has a significant effect on the arrival times and amplitudes of both P- and S-wave signals. In the following, these effects were quantified, and a parametric analysis was performed based on the physical and geometrical properties of the fracture.

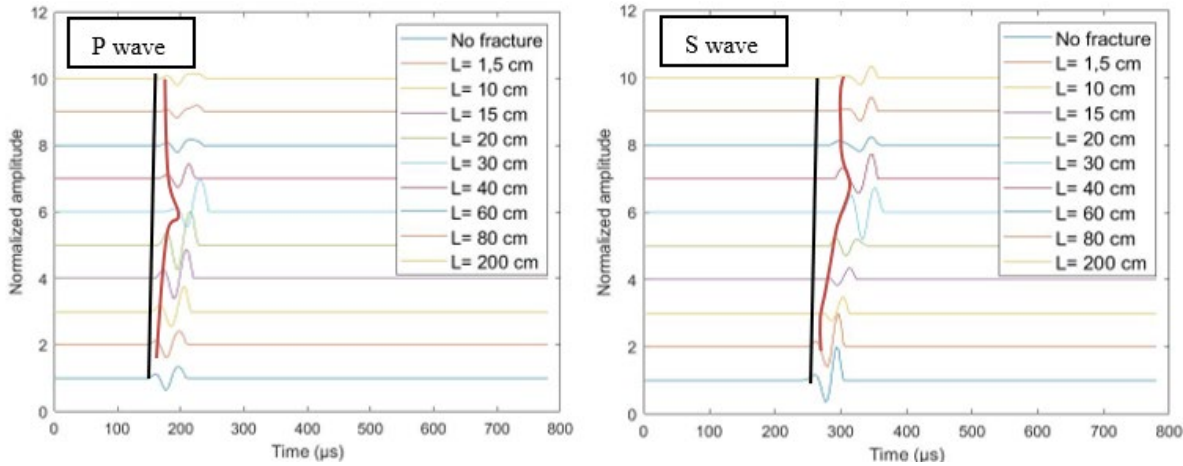


Fig. 3: Examples of extracted P and S waves for different lengths of fractures ($V_P=2000$ m/s; $V_S=750$ m/s; $RHO=1600$ kg/m³; $e=5$ cm). Red dashed line represents the first arrivals of P and S waves for fractured medium, and the black one represents the first arrivals of the reference case.

3. Results and discussion

As shown in Fig. 4a, the attenuation parameter for the S-wave is higher than that of the P-wave for all the parametric study. $\gamma_{(S)}$ is approximately constant at around 10 dB, regardless of fracture width $\gamma_{(P)}$ sharply increases up to a width smaller than 1cm, after which there is a steady response of about 6 dB (Fig. 4a). Note that the slight decrease in $\gamma_{(P)}$ and $\gamma_{(S)}$ for larger fractures is in the order of the estimation error, which is around 1dB. Fig. 4b shows that when L grows, the $\gamma_{(P)}$ drops until it reaches a value comparable to the compression wavelength (30cm). Then, there is a rise in the $\gamma_{(P)}$ until L equals twice the compression wavelength (62 cm), then the response remains stable. There is an influence of the S wave wavelength on the response for $\gamma_{(S)}$, which increases as L approaches the shear wavelength (18cm). After that, there is a drop until L reaches twice the shear wavelength. Next, the response of $\gamma_{(S)}$ is comparable to $\gamma_{(P)}$. In addition, Fig. 4c shows that as VP of fracture filling increases (i.e., the fracture becomes stiffer), $\gamma_{(P)}$ decreases, following a linear relationship. It can also be observed that $\gamma_{(S)}$ remains steady as VP increases because this amplitude decays depends on the shear modulus of the fracture infill material. We see the opposite of the previous response in Fig. 4d. Finally, when RHO increases, γ decreases. We distinguish a linear relation between RHO and $\gamma_{(P)}$ and $\gamma_{(S)}$.

The velocity variation parameter also exhibits larger changes for S-waves than for P-waves (Fig. 5a). We can see that e and $VV_{(P;S)}$, shows a quasi-linear relationship, in which $VV_{(P-S)}$ increases with e as the fracture effective compliance increases with its width. Fig. 5b shows that $VV_{(P;S)}$ increases until L approaches the compressional wavelength, then it stabilizes when L is higher than twice the compressional wavelength (Fig. 3). Fig. 5c and d show that stiffer fracture infilling material causes $VV_{(P)}$ and $VV_{(S)}$ to decrease. We also see that changes in VP affect $VV_{(S)}$ (~7%). However, when VS varies, there is no influence on P-wave response, because P waves arrive before S waves. Finally, when RHO changes, $VV_{(P;S)}$ stays constant (Fig. 5e).

From Fig. 4 and 5, we investigated a linearity between some of the fracture properties and the transmission loss factors with a high coefficient of determination ($R^2 > 0.9$). Which may help in characterizing the filled fracture properties.

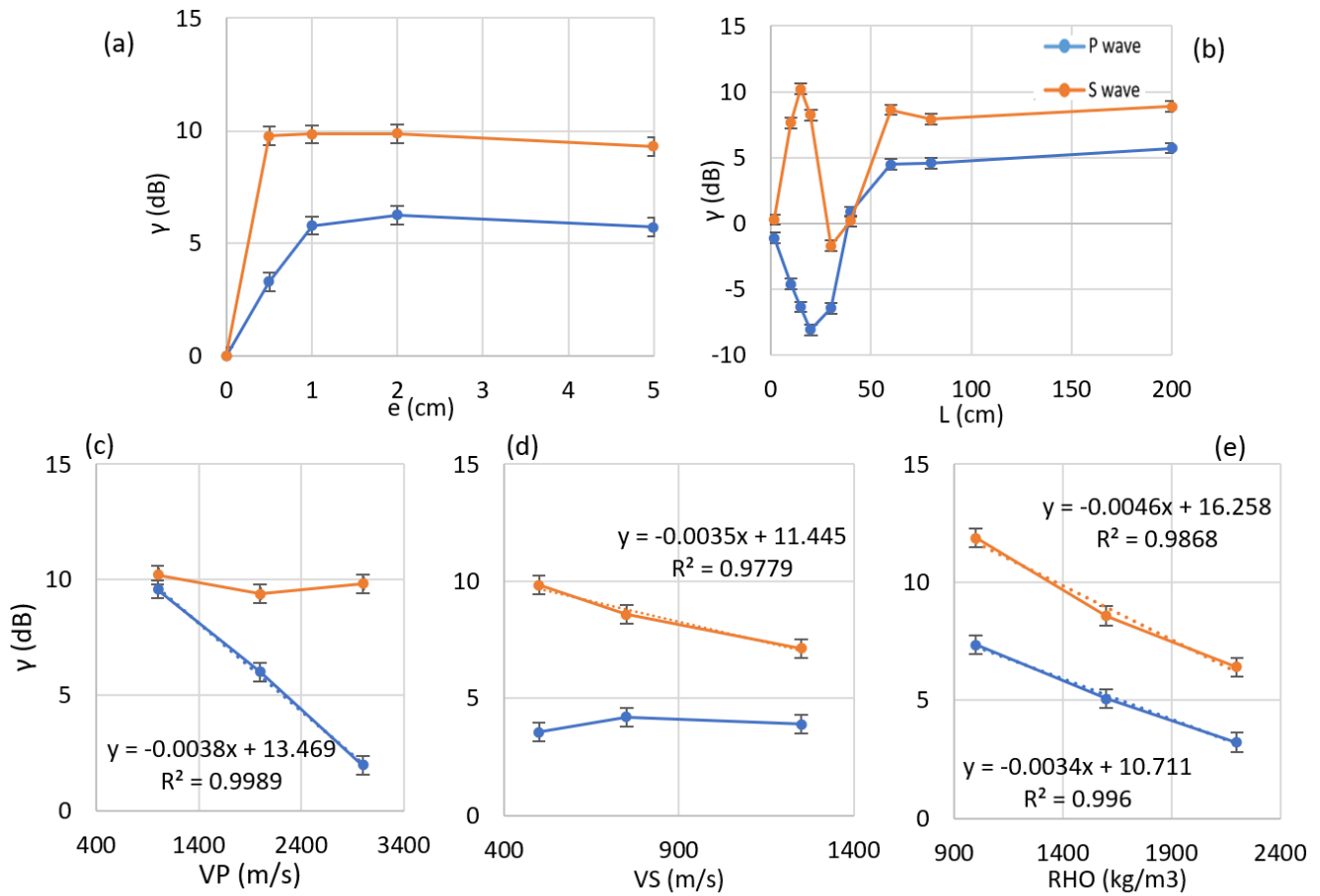


Fig. 4: The relationship between the attenuation parameter (for P and S wave) and the parameters of the parametric study. ((a) e , (b) L , (c) VP , (d) VS and (e) RHO).

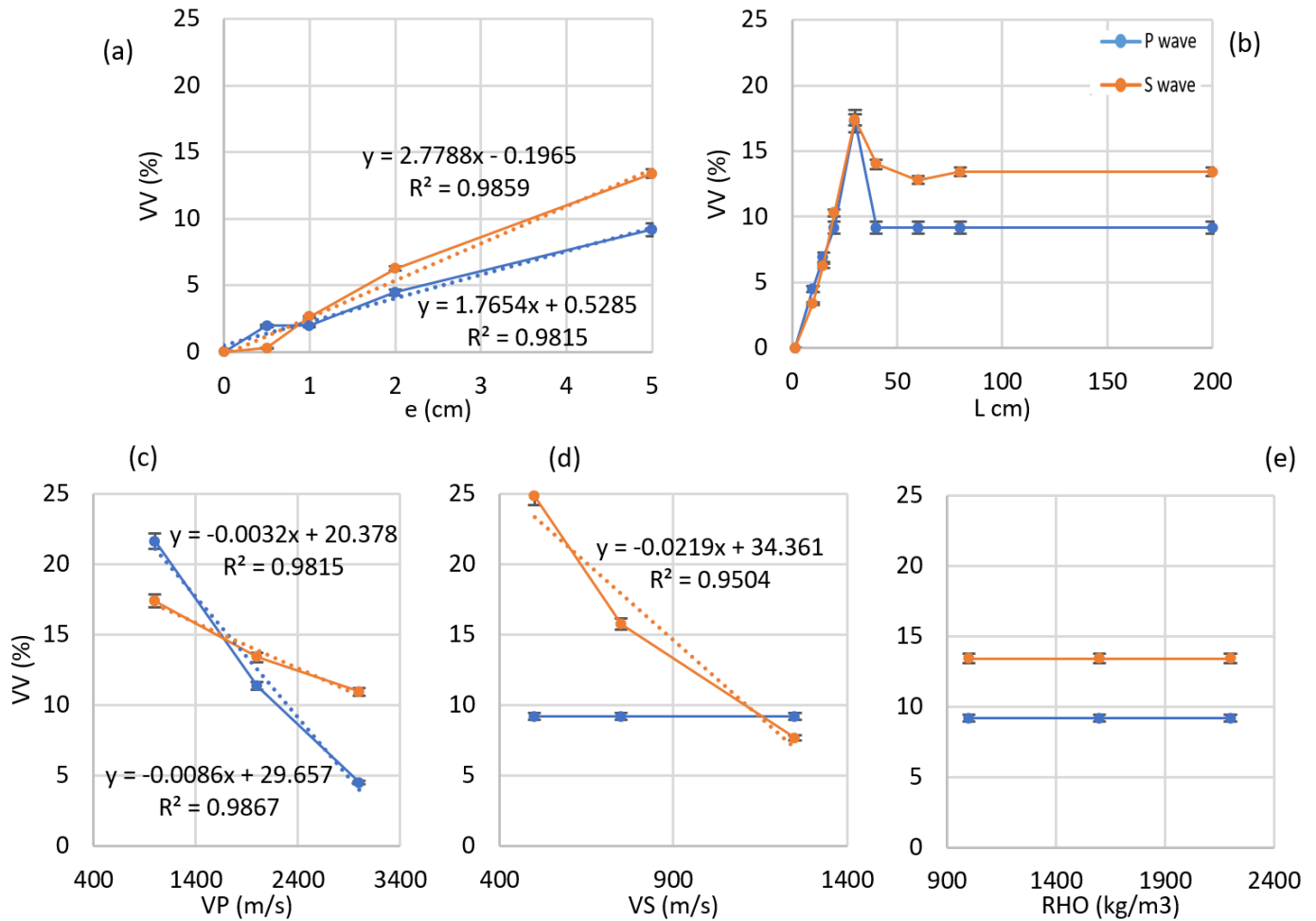


Fig. 5: The relationship between the velocity variation (for P and S wave) and the parameters of the parametric study. ((a) e, (b) L, (c) VP, (d) VS and (e) RHO).

4. Conclusion

A full-waveform numerical simulation of a borehole environment was performed to study the sensitivity of the P- and S-wave response to the mechanical and geometrical properties of a fracture. The attenuation parameter and the velocity variation were used to quantify and compare the effects.

The following conclusions are drawn based on the simulation results:

- S-waves are more sensitive to the presence and characteristics of a fracture than P-waves.
- Fracture width and VV present a quasi-linear relationship when the fracture width increases VV increases.
- For relatively thick fractures ($e > 1$ cm), it is difficult to determine the fracture width from the attenuation parameter of shear and compression waves.
- Transmission factors are affected by the fracture length, for a length lower than the radius of investigation of the FW sonic probe (~ 1 m).
- The velocity variation factor could provide information on the width and length of the fracture, as well as the fracture infill velocities.

- Fracture filling density has no significant effect on the velocity variation parameters. But can be studied through the linear relation with amplitude attenuation factors (of P and S waves).

A full parametric study will be performed to complete this work by changing the parameters of the rock matrix to create a large database.

Acknowledgements

This study has been funded by the Université de Bordeaux and MITACS. We'd like to thank René Christensen for his valuable guidance and assistance.

References

- [1] JL. Durville, and H. Héraud, “*Description des roches et des massifs rocheux*. Techniques de l’ingénieur : Construction et travaux publics : Mécanique des sols et géotechnique,” 1997. Réf. : C352 V1.
- [2] R. Lagabrielle, (2007), “Diagraphies et géophysique de forage. Techniques de l’ingénieur : Construction et travaux publics : Mécanique des sols et géotechnique,” 2007. Réf. : C225 V3.
- [3] JF. Lataste, (2011). “Contrôle Non Destructif des ouvrages d’arts : Un point de vue français sur l’organisation, les besoins et les développements en cours,”.
- [4] E. Taillet “Caractérisation des discontinuités dans des ouvrages massifs en béton par la diagraphie électrique de résistivité,” Ph.D. dissertation, Sherbrooke Univ., Quebec, Canada, and Bordeaux Univ.,Bordeaux, France, 2013.
- [5] P. Thivierge, “Caractérisation des infrastructures à l’aide des diagraphies d’imagerie optique et acoustique.” Thèse de maîtrise de l’université de Sherbrooke, 185 pages. M.Sc. dissertation, Sherbrooke Univ., Quebec, Canada, 2011.
- [6] F.D. Day-Lewis, L. D. Slater, J. Robinson, C. D. Johnson, N. Terry, D. Werkema, (2017). “An overview of geophysical technologies appropriate for characterization and monitoring at fractured-rock sites” *Journal of Environmental Management*, Volume 204, Part 2. <https://doi.org/10.1016/j.jenvman.2017.04.033>.
- [7] B. Yan, W. Ou, X. Huang, and NV. Da Silva, (2020). “Numerical simulation of shear wave attenuation in borehole inserted by a horizontal fracture”. *Acta Geophysica*. <https://doi.org/10.1007/s11600-020-00503-3>
- [8] R. L. Morris, D. R. Grine, and T. E. Arkfeld, (1964). “Using compressional and shear acoustic amplitudes for the location of fractures”.*Journal of Petroleum Technology*, 16, 623–632.
- [9] Pyrak-Nolte, L. J., Myer, L. R., & Cook, N. G. W., (1990). “Transmission of seismic waves across single natural fractures”. *Journal Geophysical Research*, 95, 8617–8638.
- [10] N. Barbosa, E. Caspari, G. Rubino, A. Greenwood, L. Baron, and K. Holliger, (2019). “Estimation of Fracture Compliance From Attenuation and Velocity Analysis of Full-Waveform Sonic Log Data,” *Journal of Geophysical Research: Solid Earth*. 10.1029/2018 E. JB016507.
- [11] N. Barbosa, A. Greenwood, E. Caspari, N. Dutler, K. Holliger, (2021). “Estimates of Individual Fracture Compliances Along Boreholes From Full-Waveform Sonic Log Data,” *Journal of Geophysical Research: Solid Earth*. 10.1029/2021JB022015.
- [12] Comsol (2012). *Mechanics module user’s guide*, version 4.3. U.S. Patents 7,519,518; 7,596,474; and 7,623,991. Patents pending.
- [13] T. Wang, and X. Tang, (2003). “Finite-difference modeling of elastic wave propagation: a nonsplitting perfectly matched layer approach”. *Geophysics* 68(5):1749–1755, 2003.
- [14] Molyneux, J. B., and Schmitt, D. R, (2000). *Compressional-wave velocities in attenuating media: A laboratory physical model study*. *Geophysics*, 65, 1162–1167.